

Published in final edited form as:

Curr Biol. 2014 October 6; 24(19): 2288–2294. doi:10.1016/j.cub.2014.08.012.

An assay for clogging the ciliary pore complex distinguishes mechanisms of cytosolic and membrane protein entry

Daisuke Takao, John F Dishinger, H Lynn Kee, Justine M Pinskey, Ben L Allen, and Kristen J Verhey

Department of Cell Biology, University of Michigan Medical School, Ann Arbor, MI 48109

Kristen J Verhey: kjverhey@umich.edu

Summary

As a cellular organelle, the cilium contains a unique protein composition [1, 2]. Entry of both membrane [3–5] and cytosolic components [6–8] is tightly regulated by gating mechanisms at the cilium base, however, the mechanistic details of ciliary gating are largely unknown. We previously proposed that entry of cytosolic components is regulated by mechanisms similar to those of nuclear transport and is dependent on nucleoporins (NUPs) which comprise a ciliary pore complex (CPC) [6, 9]. To investigate ciliary gating mechanisms, we developed a system to clog the pore by inhibiting NUP function via forced dimerization. We targeted NUP62, a component of the central channel of the nuclear pore complex (NPC) [10], for forced dimerization by tagging it with the homodimerizing Fv domain. As proof of principle, we show that forced dimerization of NUP62-Fv attenuated active transport of bovine serum albumin into the nuclear compartment and of the kinesin-2 motor KIF17 into the ciliary compartment. Using the pore clogging technique, we find that forced dimerization of NUP62 attenuated the gated entry of cytosolic proteins but did not affect entry of membrane proteins or diffusional entry of small cytosolic proteins. We propose a model in which active transport of cytosolic proteins into both nuclear and ciliary compartments requires functional NUPs of the central pore whereas lateral entry of membrane proteins utilizes a different mechanism that is likely specific to each organelle's limiting membrane.

Results and Discussion

A system of forced dimerization of NUP62 disrupts active transport through the NPC and CPC

To investigate the role of the CPC in ciliary gating mechanisms, we developed a system to specifically disrupt CPC function in mammalian cells. We reasoned that forced dimerization

© 2014 Elsevier Inc. All rights reserved.

Publisher's Disclaimer: This is a PDF file of an unedited manuscript that has been accepted for publication. As a service to our customers we are providing this early version of the manuscript. The manuscript will undergo copyediting, typesetting, and review of the resulting proof before it is published in its final citable form. Please note that during the production process errors may be discovered which could affect the content, and all legal disclaimers that apply to the journal pertain.

Additional Experimental Procedures can be found in the Supplementary Information.

Author Contributions

DT, JFD, BLA, and KJV designed experiments. DT, JFD, HLK, and JMP carried out experiments. DT and KJV wrote the manuscript with input from all authors.

of core NUPs of the CPC would restrict their mobility and clog the pore. We thus tagged core NUPs with the modified FKBP domain Fv (also known as DmrB) and induced dimerization by addition of the homodimerizing drug Rapalog-2 [also known as B/B homodimerizer and referred to hereafter as homodimerizer (HD)]. A similar method was recently used to block the NPC in yeast cells by engineering a central NUP with a binding motif (dynein light chain-interacting domain) for a large protein, Dyn2 [11]. Transcriptional upregulation of the engineered NUP plugged the pore and blocked nucleocytoplasmic transport. Our system has the advantage of rapid induction via drug addition.

The nucleoporin NUP62 is a functional component of the central pore of the NPC (Figure 1A, [10]) and also localizes to the CPC at the ciliary base [6]. We created four constructs in which the Fv domain was placed at the N-terminus, C-terminus or two different internal regions of NUP62 (Figure S1A) using a previously-described NUP62-EGFP3 construct (Figure S1B, [6, 12]) as a backbone. When expressed in NIH 3T3 cells, the Fv-NUP62 constructs localized to the nuclear envelope as well as to the base of the cilium (Figure S1C,E), as expected. These results indicate that fusion of an Fv domain or a fluorescent protein tag does not affect NUP62 localization.

The ability of the Fv-NUP62 constructs to clog the NPC upon forced dimerization was tested by measuring the nuclear import of rhodamine-labeled bovine serum albumin containing a nuclear localization sequence (rhod-BSA-NLS). Only the C-terminally tagged NUP62 construct, NUP62-Fv-EGFP3 fulfilled the criteria of allowing nucleocytoplasmic transport in the absence of HD and blocking transport in the presence of HD (Figures 1C, 1D and summarized in Figure S1A). Forced dimerization of NUP62-Fv-EGFP3 also attenuated corticosterone-induced nuclear import of the HIV-1 transactivating protein Rev fused to the hormone-binding region of the glucocorticoid receptor (Gr) and GFP (Rev-Gr-GFP, [13]) (Figure S2A, S2B). Although the mechanism underlying the differences between the Fv-NUP62 constructs is unclear, it is likely that domain location and/or orientation within the NPC [14] affects the ability of the Fv-NUPs to clog the NPC. Consistent with this, recent work using rapamycin-induced FKBP-FRB heterodimerization to link NUPs and transport cargoes suggested that the efficiency of the linkage is dependent on the transport cargo [15].

The ability of the NUP62-Fv construct to clog the CPC upon forced dimerization was tested by measuring ciliary import of the kinesin-2 family member KIF17 whose entry into the ciliary compartment is known to be regulated by NUPs of the CPC [6]. We used a Cerulean (Cer)-tagged version of NUP62-Fv (Figure 1B, Figure S1C) and measured ciliary import of KIF17 using fluorescence recovery after photobleaching (FRAP) in cells expressing KIF17-mCit with the ciliary marker Arl13b-mCherry (Figure 1E). KIF17-mCit in the ciliary tip was photobleached and the fluorescence recovery was measured in the absence and presence of HD. In control cells, KIF17-mCit fluorescence recovered over 30 min due to the entry of new KIF17-mCit molecules from the cytosol into the cilium (Figures 1F and 1G). In the presence of HD, the FRAP rate was significantly decreased (Figure 1G). Forced dimerization of NUP62-Fv did not cause long-term effects such as a reduced population of ciliated cells (data not shown), presumably due to incomplete blockage of ciliary entry. Addition of HD did not affect the fluorescence recovery of KIF17-mCit in cells not

expressing NUP62-Fv (Figure S2C) or in cells expressing NUP62-Cer (no Fv domain, Figure S2D), indicating that decreased ciliary entry upon pore clogging was not due to non-specific effects of HD. These results demonstrate that forced dimerization of NUP62-Fv attenuates the gated entry of ciliary proteins, presumably by clogging the CPC.

Taken together, these results suggest that NUP62 of the CPC is involved in active transport of cytosolic proteins into both the ciliary and nuclear compartments. To test whether central NUPs are also involved in regulating diffusive entry of cytosolic proteins into these compartments, we tested whether forced dimerization of NUP62-Fv blocked the entry of recombinant GFP (rGFP) microinjected into the cytoplasm of NIH 3T3 cells expressing NUP62-Fv-Cer. We found that after 20 min, the diffusional entry of rGFP into both the nucleus and the cilium was not altered by addition of HD and clogging of the central pore (Figure 2). Although there may be effects on the dynamics of rGFP entry not measured in our assay, these results are consistent with the finding that disrupting NUPs does not affect diffusional passage of small molecules through the NPC [16–18]. Thus, forced dimerization of NUP62-Fv specifically disrupts NUP62-dependent active transport mechanisms in both the NPC and the CPC, while it does not affect NUP62-independent transport such as diffusion.

Forced dimerization of NUP62-Fv attenuates gated entry of cytosolic proteins into the cilium

Having established the use of NUP62-Fv as a tool to attenuate active transport of cytosolic molecules into the nuclear and ciliary compartments, we used this approach to examine the role of nucleoporins of the CPC in ciliary gating. We initially tested whether forced dimerization of NUP62-Fv could disrupt ciliary import of cytosolic proteins.

Gli2 is a transcription factor of the Hedgehog signaling pathway [19, 20]. When expressed in NIH 3T3 cells, GFP-Gli2 localized to the tip of the cilium. In the absence of HD, GFP-Gli2 fluorescence recovered up to ~40% in 40 min and in the presence of HD, this fluorescence recovery was significantly reduced (Figures 3A and S3A). These results indicate that forced dimerization of NUP62-Fv inhibits ciliary entry of GFP-Gli2, suggesting that ciliary entry of Gli2, similar to KIF17, is regulated by NUP62-dependent mechanisms.

Tsga14 (also known as CEP41) and Gtl3 (a homolog of *Chlamydomonas* BUG22) were recently identified as ciliary proteins by proteomic analysis of cilia isolated from a kidney cell line [21]. When expressed in NIH 3T3 cells, Tsga14-GFP localized along the entire cilium (Figure 3B) whereas Gtl3-GFP was more enriched in the basal region (Figure 3C), as previously described [21]. Their average fluorescence intensities along the cilium were measured for FRAP analysis. In the absence of HD, fluorescence of Tsga14-GFP recovered up to ~60% in 20 min (Figures 3B and S3B) while that of Gtl3-GFP recovered up to ~80% in 30 min (Figure 3C and S3C). In the presence of HD, the FRAP of both Tsga14-GFP and Gtl3-GFP was significantly decreased (Figures 3B and 3C), suggesting that ciliary entry of these proteins is regulated by NUP62-dependent mechanisms.

Intraflagellar transport (IFT) is a crucial system for maintenance and function of cilia; we thus investigated whether ciliary entry of IFT components would be affected by forced

dimerization of NUP62-Fv. IFT88 and IFT20 are core or peripheral components of the anterograde IFT-B subcomplex, respectively [22, 23]. In NIH 3T3 cells stably expressing IFT88-mCit, the protein was localized to the entire cilium and almost no signal was observed in the cytoplasm or the nucleus (Figure 3D). Given previous reports of IFT88-YFP localization at the ciliary tip [24] or along the entire cilium [3] in IMCD3 cells, localization of IFT88 might differ slightly according to cell types and/or experimental conditions. For IFT20-GFP, low levels of fluorescence were detected along the entire cilium in NIH 3T3 cells (Figure 3E), similar to previous results in IMCD3 cells [25]. In control FRAP experiments, both IFT88-mCit and IFT20-GFP fluorescence recovered up to ~80% in 30 min (Figure 3D,E and Figure S3D,E). Interestingly, in the presence of HD, the FRAP of IFT88-mCit was significantly decreased whereas that of IFT20-GFP was not affected (Figures 3D and 3E). In summary, these results suggest that NUPs of the CPC are involved in ciliary import of most cytosolic proteins into the ciliary compartment.

That ciliary entry of cytosolic proteins utilizes molecules and mechanisms of nuclear transport was previously shown for the kinesin-2 motor KIF17 [6, 9]. We now extend these results to show that central NUP proteins regulate the ciliary entry of a variety of cytosolic proteins, ranging from transcription factors (Gli2 and potentially Gtl3) to IFT particle components (IFT88). Interestingly, only IFT20-GFP displayed ciliary transport properties that were not blocked by forced dimerization of NUP62-Fv (Figure 3E). IFT20 is thought to be a peripheral component of the IFT-B subcomplex [23] and has been proposed to play a role in sorting of ciliary proteins at the Golgi complex [25–29]. Thus, IFT20-GFP could gain access to the cilium via its interaction with membrane proteins rather than as a cytosolic IFT component. Alternatively, IFT20-GFP could enter the cilium by passive diffusion as its small size (~15 kDa), even when fused with GFP (~27 kDa), is below the size-exclusion limit of the ciliary barrier [6–8].

Forced dimerization of NUP62-Fv has no effect on gating of membrane proteins into and out of the ciliary compartment

We next used forced dimerization of NUP62-Fv to test whether nucleoporins of the CPC play a role in regulating ciliary entry of membrane proteins. For peripheral membrane proteins, we used mCitrine tagged with a dual palmitoylation sequence (PalmPalm-mCit) and retinitis pigmentosa 2 (RP2) tagged with GFP (RP2-GFP). Palmitoylation provides a point of membrane association [22], resulting in targeting of mCitrine to both the ciliary and plasma membranes (Figure 4A). RP2-GFP was also localized to ciliary and plasma membranes (Figure 4B), as previously described [30]. The FRAP rates of these proteins were more rapid (~80% recovery in 5 min, Figures 4A,B and Figures S3F,G), compared to those of the cytosolic proteins (20 min or more to reach plateau, Figure 3). Import of PalmPalm-mCit was not affected by forced dimerization of NUP62-Fv (Figure 4A) whereas that of RP2-GFP was only slightly affected at early time points (Figure 4B). That ciliary entry of RP2 was unaffected by forced dimerization of NUP62-Fv was surprising as the importin-Ran system has been shown to regulate ciliary entry of RP2 [30]. It is possible that the small size and membrane anchor of RP2 enable it to bypass the pore clogging induced by forced dimerization of NUP62-Fv. We conclude that ciliary entry of the peripherally

membrane-associated proteins PalmPalm-mCit and RP2-GFP is largely independent of NUP62.

We then tested if transport of transmembrane proteins into cilia is affected by forced dimerization of NUP62-Fv. A number of studies have documented that transmembrane proteins show little to no fluorescence recovery in FRAP experiments [3, 5, 8, 24] and we also found this to be true for the somatostatin receptor 3 (Sstr3, data not shown). Thus, we utilized a mutant form of Smoothed (SmoM2) which constitutively localizes to the ciliary membrane in the absence of Hedgehog ligand [31]. The fluorescence recovery of SmoM2-YFP was very low (~30% in 30 min, Figures 4C and S3H) and was unaffected by the addition of HD (Figure 4C). These results suggest that ciliary entry of SmoM2 is independent of NUP62.

To further explore the role of NUP62 in gating transport of transmembrane proteins between the cell body and the ciliary compartment, we tested whether the Hedgehog-dependent movement of several transmembrane proteins was affected by forced dimerization of NUP62-Fv. First, the Hedgehog-dependent entry of Smo was analyzed by staining untreated and HD-treated cells with an antibody to the endogenous Smo protein. Addition of Sonic hedgehog (Shh) induced the ciliary localization of Smo protein [32], a transport process that was not altered by forced dimerization of NUP62-Fv (Figure 4D and Figure S4A). Second, we tested the Hedgehog-dependent ciliary exit of the Hedgehog receptor Patched (Ptch1) and the orphan G-protein-coupled receptor Gpr161. The amount of Ptch1 protein in the ciliary compartment was increased by treating cells with SAG; ciliary exit was then stimulated by Shh treatment (Figure 4E and Figure S4B; [33]). Gpr161-mCit localized to the ciliary compartment when expressed in NIH 3T3 cells, but was exported upon exposure to SAG or Shh (Figure 4F and Figure S4C; [34]). Forced dimerization of NUP62-Fv-Cer did not affect the ciliary exit of either endogenous Ptch1 (Figure 4E, Figure S4B) or expressed Gpr161-mCit (Figure 4F, Figure S4C) proteins. Taken together, in contrast to the case of cytosolic proteins, forced dimerization of NUP62-Fv does not appear to affect ciliary transport of peripheral membrane or transmembrane proteins.

Our results provide the first analysis of NUP function in the gating of membrane proteins into and out of the ciliary compartment. Our finding that ciliary gating of membrane proteins is independent of CPC function has two broad implications. First, our results provide a unifying theme for the field in suggesting that ciliary entry of cytosolic proteins requires NUPs of the CPC whereas ciliary entry of membrane proteins is regulated by alternative mechanisms that presumably involve proteins of the transition zone whose functions are compromised in ciliopathies [35, 36]. Second, these results further extend the parallels between ciliary and nuclear import processes as nuclear import of transmembrane proteins is largely independent of central components of the NPC [37, 38].

Distinct pathways for ciliary transport according to the class of proteins

Entry into the cilium is a gated process that requires distinct molecules and mechanisms. By developing a novel system to specifically block NUP-based barriers, we investigated the role of central pore nucleoporins in regulating ciliary entry. Diffusional entry of small cytosolic proteins into the ciliary and nuclear compartments was not affected by disrupting NUP62

function at the CPC or NPC, respectively, consistent with previous work [6–8, 16–18]. We show that ciliary entry of most cytosolic proteins was attenuated by forced dimerization of NUP62-Fv. Thus, we propose that ciliary entry of cytosolic proteins, including IFT motors and particles, occurs via a NUP-containing channel at the ciliary base. This is similar to nuclear transport where entry of cytosolic proteins requires active transport processes that utilize a functional central channel within the NPC [39–41]. We show that in contrast to cytosolic proteins, ciliary gating of membrane proteins was unperturbed by forced dimerization of NUP62-Fv, suggesting that ciliary gating of membrane proteins involves a distinct transport pathway that likely utilizes molecules of the transition zone [35, 36]. Likewise, the lateral entry of membrane proteins into the nuclear compartment is largely independent of the central pore and may utilize peripheral channels in the NPC [37, 38]. Although this work extends the parallels between nuclear and ciliary import processes, further work is required to decipher the hierarchy of signals and molecular interactions that mediate targeting to the ciliary base, transport across the ciliary barrier, and transport within the ciliary compartment. For example, ciliary import of RP2 is regulated by importin- β 2 [30] yet appears to be independent of NUP62 function, indicating a multi-layered complexity to ciliary gating mechanisms.

Our results open up new questions about how IFT motors and their cargoes cross the ciliary gate. For example, are kinesin motors and IFT particles required for trafficking of membrane proteins into and/or within the ciliary compartment? We propose that ciliary entry of cytosolic proteins is both IFT- and NUP-dependent whereas membrane proteins cross the ciliary barrier independent of IFT particles and central NUPs of the CPC. This proposal is consistent with recent studies demonstrating that entry of phospholipase D, a peripheral membrane protein, and SAG1, a transmembrane protein, into cilia is independent of IFT [42, 43] and that movement of transmembrane proteins within the ciliary membrane is also largely independent of IFT [44]. Also, it is interesting to note that recent evidence using cryoelectron microscopy has identified pores at the ciliary base in *Tetrahymena* and these pores may be the sites where the CPCs are localized [45]. The NUP composition and structural organization of these pores may differ from that of the NPC as no membrane structure is thought to surround the pores at the cilium base. Further investigation into both the structural and functional basis of the CPC will provide insights for cilium-specific gating mechanisms.

Experimental Procedures

Drug treatments

To induce forced dimerization of NUP62-Fv, 1.5 μ M B/B homodimerizer (Clontech) was added to culture medium for 2 h before experiments. For corticosterone-induced nuclear import of Rev-Gr-GFP, cells were transfected with Rev-Gr-GFP and NUP62-Fv-Cer for 24h, treated with HD or vehicle (ethanol) for 2 h, and then 1 μ M corticosterone was added for 60 min as previously described [13]. To assess the Hedgehog-induced redistribution of transmembrane proteins, cells were treated with Shh-containing conditioned media from NSHH-transfected (NShh-pCDNA3) COS7 cells and/or 250 nM SAG (Enzo Life Sciences). For analysis of expressed and endogenous Smo, cells were serum-starved for 24 h, treated

with HD or vehicle (ethanol) for 2 h, and then Shh-conditioned medium was added for 2 h before fixation and staining. For analysis of endogenous Ptch, cells were serumstarved for 24 h and then incubated with SAG in serum-free media for 24 h. After a 2 h incubation with HD or ethanol, Shh-conditioned medium was added for 4 h, and then the cells were fixed and stained. For analysis of transfected Gpr161-mCit, cells were serum-starved for 24 h, treated with HD or ethanol for 2 h, and then either 0.1% (v/v) DMSO, Shh-conditioned medium or SAG was added to medium. After 24 h incubation, the cells were fixed and stained. Flow diagrams of these experiments are shown in Figure S4.

FRAP

FRAP experiments and analyses were performed as described [46]. A Nikon A1 confocal system with 60× water immersion objective (N.A. 1.20) was used. A stage-top incubator (Tokai Hit) was used to maintain cells at 37°C and 5% CO₂. Three sequential images were taken and then the fluorescently-tagged ciliary protein of interest was photobleached with the lowest laser power required for photobleaching (varied depending on construct). Fluorescence images were obtained for both Arl13b-mCherry and the EGFP- or mCit-labeled proteins and the Arl13b-mCherry images were used to ensure the position of the cilium during imaging and post-imaging quantification. The focus was adjusted between image acquisitions when a cilium seemed to be going away from the focal plane (typically once every 10 min). Fluorescence intensities were measured using Image J software (NIH). A region of interest (ROI) was selected to include all signal in the cilium; circular ROIs were used for KIF17-mCit and GFP-Gli2 that are localized in the ciliary tip, while segmented line ROIs (2–3 pixels in width) were used for proteins that localized along the cilium. After background subtraction, the fluorescence intensities of the ROI were normalized against the averaged intensities of the three pre-photobleaching images. Normalized fluorescence intensities at each time point were compared between the absence and presence of HD by t-test.

Supplementary Material

Refer to Web version on PubMed Central for supplementary material.

Acknowledgments

This work was supported by an award to KJV from the NIH National Institute of General Medical Sciences (R01GM070862). DT was supported by a Postdoctoral Fellowship for Research Abroad from the Japan Society for the Promotion of Science. BLA was supported by awards from the NIH (R21CA167122) and American Heart Association (11SDG6380000). We gratefully acknowledge S. Lentz and the Morphology and Image Analysis Core of the Michigan Diabetes Research and Training Center funded by NIH5P60DK20572 from the National Institute of Diabetes & Digestive & Kidney Diseases.

References

1. Goetz SC, Anderson KV. The primary cilium: a signalling centre during vertebrate development. *Nat. Rev. Genet.* 2010; 11:331–344. [PubMed: 20395968]
2. Hildebrandt F, Benzing T, Katsanis N. Ciliopathies. *N. Engl. J. Med.* 2011; 364:1533–1543. [PubMed: 21506742]

3. Hu Q, Milenkovic L, Jin H, Scott MP, Nachury MV, Spiliotis ET, Nelson WJ. A septin diffusion barrier at the base of the primary cilium maintains ciliary membrane protein distribution. *Science*. 2010; 329:436–439. [PubMed: 20558667]
4. Garcia-Gonzalo FR, Corbit KC, Sireerol-Piquer MS, Ramaswami G, Otto Ea, Noriega TR, Seol AD, Robinson JF, Bennett CL, Josifova DJ, et al. A transition zone complex regulates mammalian ciliogenesis and ciliary membrane composition. *Nat. Genet.* 2011; 43:776–784. [PubMed: 21725307]
5. Chih B, Liu P, Chinn Y, Chalouni C, Komuves LG, Hass PE, Sandoval W, Peterson AS. A ciliopathy complex at the transition zone protects the cilia as a privileged membrane domain. *Nat. Cell Biol.* 2012; 14:61–72. [PubMed: 22179047]
6. Kee HL, Dishinger JF, Blasius TL, Liu C-J, Margolis B, Verhey KJ. A size-exclusion permeability barrier and nucleoporins characterize a ciliary pore complex that regulates transport into cilia. *Nat. Cell Biol.* 2012; 14:431–437. [PubMed: 22388888]
7. Lin Y-C, Niewiadomski P, Lin B, Nakamura H, Phua SC, Jiao J, Levchenko A, Inoue T, Rohatgi R, Inoue T. Chemically inducible diffusion trap at cilia reveals molecular sieve-like barrier. *Nat. Chem. Biol.* 2013; 9:437–443. [PubMed: 23666116]
8. Breslow DK, Koslover EF, Seydel F, Spakowitz AJ, Nachury MV. An in vitro assay for entry into cilia reveals unique properties of the soluble diffusion barrier. *J. Cell Biol.* 2013; 203:129–147. [PubMed: 24100294]
9. Dishinger JF, Kee HL, Jenkins PM, Fan S, Hurd TW, Hammond JW, Truong YN-T, Margolis B, Martens JR, Verhey KJ. Ciliary entry of the kinesin-2 motor KIF17 is regulated by importin-beta2 and RanGTP. *Nat. Cell Biol.* 2010; 12:703–710. [PubMed: 20526328]
10. Strambio-De-Castillia C, Niepel M, Rout MP. The nuclear pore complex: bridging nuclear transport and gene regulation. *Nat. Rev. Mol. Cell Biol.* 2010; 11:490–501. [PubMed: 20571586]
11. Stelter P, Kunze R, Fischer J, Hurt E. Probing the nucleoporin FG repeat network defines structural and functional features of the nuclear pore complex. *J. Cell Biol.* 2011; 195:183–192. [PubMed: 21987633]
12. Rabut G, Doye V, Ellenberg J. Mapping the dynamic organization of the nuclear pore complex inside single living cells. *Nat. Cell Biol.* 2004; 6:1114–1121. [PubMed: 15502822]
13. Love DC, Sweitzer TD, Hanover JA. Reconstitution of HIV-1 rev nuclear export: independent requirements for nuclear import and export. *Proc. Natl. Acad. Sci. U. S. A.* 1998; 95:10608–10613. [PubMed: 9724751]
14. Solmaz SR, Chauhan R, Blobel G, Melák I. Molecular architecture of the transport channel of the nuclear pore complex. *Cell.* 2011; 147:590–602. [PubMed: 22036567]
15. Patury S, Geda P, Dobry CJ, Kumar A, Gestwicki JE. Conditional nuclear import and export of yeast proteins using a chemical inducer of dimerization. *Cell Biochem. Biophys.* 2009; 53:127–134. [PubMed: 19159085]
16. Finlay DR, Newmeyer DD, Price TM, Forbes DJ. Inhibition of in vitro nuclear transport by a lectin that binds to nuclear pores. *J. Cell Biol.* 1987; 104:189–200. [PubMed: 3805121]
17. Yoneda Y, Imamoto-Sonobe N, Yamaizumi M, Uchida T. Reversible inhibition of protein import into the nucleus by wheat germ agglutinin injected into cultured cells. *Exp. Cell Res.* 1987; 173:586–595. [PubMed: 2446896]
18. Mohr D, Frey S, Fischer T, Güttler T, Görlich D. Characterisation of the passive permeability barrier of nuclear pore complexes. *EMBO J.* 2009; 28:2541–2553. [PubMed: 19680228]
19. Eggenschwiler JT, Anderson KV. Cilia and developmental signaling. *Annu. Rev. Cell Dev. Biol.* 2007; 23:345–373. [PubMed: 17506691]
20. Simpson F, Kerr MC, Wicking C. Trafficking, development and hedgehog. *Mech. Dev.* 2009; 126:279–288. [PubMed: 19368798]
21. Ishikawa H, Thompson J, Yates JR, Marshall WF. Proteomic analysis of mammalian primary cilia. *Curr. Biol.* 2012; 22:414–419. [PubMed: 22326026]
22. Hsiao Y-C, Tuz K, Ferland RJ. Trafficking in and to the primary cilium. *Cilia.* 2012; 1:4. [PubMed: 23351793]
23. Sung C-H, Leroux MR. The roles of evolutionarily conserved functional modules in cilia-related trafficking. *Nat. Cell Biol.* 2013; 15:1387–1397. [PubMed: 24296415]

24. Larkins CE, Aviles GDG, East MP, Kahn Ra, Caspary T. Arl13b regulates ciliogenesis and the dynamic localization of Shh signaling proteins. *Mol. Biol. Cell.* 2011; 22:4694–4703. [PubMed: 21976698]
25. Follit JA, Tuft RA, Fogarty KE, Pazour GJ. The intraflagellar transport protein IFT20 is associated with the Golgi complex and is required for cilia assembly. *Mol. Biol. Cell.* 2006; 17:3781–3792. [PubMed: 16775004]
26. Baker, Sa; Freeman, K.; Luby-Phelps, K.; Pazour, GJ.; Besharse, JC. IFT20 links kinesin II with a mammalian intraflagellar transport complex that is conserved in motile flagella and sensory cilia. *J. Biol. Chem.* 2003; 278:34211–34218. [PubMed: 12821668]
27. Follit, Ja; Xu, F.; Keady, BT.; Pazour, GJ. Characterization of mouse IFT complex B. *Cell Motil. Cytoskeleton.* 2009; 66:457–468. [PubMed: 19253336]
28. Keady BT, Le YZ, Pazour GJ. IFT20 is required for opsin trafficking and photoreceptor outer segment development. *Mol. Biol. Cell.* 2011; 22:921–930. [PubMed: 21307337]
29. Crouse JA, Lopes VS, Sanagustin JT, Keady BT, Williams DS, Pazour GJ. Distinct functions for IFT140 and IFT20 in opsin transport. *Cytoskeleton.* 2014; 71:302–310. [PubMed: 24619649]
30. Hurd TW, Fan S, Margolis BL. Localization of retinitis pigmentosa 2 to cilia is regulated by Importin beta2. *J. Cell Sci.* 2011; 124:718–726. [PubMed: 21285245]
31. Xie J, Murone M, Luoh SM, Ryan A, Gu Q, Zhang C, Bonifas JM, Lam CW, Hynes M, Goddard A, et al. Activating Smoothed mutations in sporadic basal-cell carcinoma. *Nature.* 1998; 391:90–92. [PubMed: 9422511]
32. Corbit KC, Aanstad P, Singla V, Norman AR, Stainier DYR, Reiter JF. Vertebrate Smoothed functions at the primary cilium. *Nature.* 2005; 437:1018–1021. [PubMed: 16136078]
33. Rohatgi R, Milenkovic L, Scott MP. Patched1 regulates hedgehog signaling at the primary cilium. *Science.* 2007; 317:372–376. [PubMed: 17641202]
34. Mukhopadhyay S, Wen X, Ratti N, Loktev A, Rangell L, Scales SJ, Jackson PK. The ciliary G-protein-coupled receptor Gpr161 negatively regulates the Sonic hedgehog pathway via cAMP signaling. *Cell.* 2013; 152:210–223. [PubMed: 23332756]
35. Czarnecki PG, Shah JV. The ciliary transition zone: from morphology and molecules to medicine. *Trends Cell Biol.* 2012; 22:201–210. [PubMed: 22401885]
36. Reiter JF, Blacque OE, Leroux MR. The base of the cilium: roles for transition fibres and the transition zone in ciliary formation, maintenance and compartmentalization. *EMBO Rep.* 2012; 13:608–618. [PubMed: 22653444]
37. Zuleger N, Kerr ARW, Schirmer EC. Many mechanisms, one entrance: membrane protein translocation into the nucleus. *Cell. Mol. Life Sci.* 2012; 69:2205–2216. [PubMed: 22327555]
38. Katta SS, Smoyer CJ, Jaspersen SL. Destination: inner nuclear membrane. *Trends Cell Biol.* 2013; 24:221–229. [PubMed: 24268652]
39. Finlay DR, Meier E, Bradley P, Horecka J, Forbes DJ. A complex of nuclear pore proteins required for pore function. *J. Cell Biol.* 1991; 114:169–183. [PubMed: 2050741]
40. Rout MP, Aitchison JD, Suprpto a, Hjertaas K, Zhao Y, Chait BT. The yeast nuclear pore complex: composition, architecture, and transport mechanism. *J. Cell Biol.* 2000; 148:635–651. [PubMed: 10684247]
41. Leng Y, Cao C, Ren J, Huang L, Chen D, Ito M, Kufe D. Nuclear import of the MUC1-C oncoprotein is mediated by nucleoporin Nup62. *J. Biol. Chem.* 2007; 282:19321–19330. [PubMed: 17500061]
42. Lechtreck KF, Brown JM, Sampaio JL, Craft JM, Shevchenko A, Evans JE, Witman GB. Cycling of the signaling protein phospholipase D through cilia requires the BBSome only for the export phase. *J. Cell Biol.* 2013; 201:249–261. [PubMed: 23589493]
43. Belzile O, Hernandez-Lara CI, Wang Q, Snell WJ. Regulated membrane protein entry into flagella is facilitated by cytoplasmic microtubules and does not require IFT. *Curr. Biol.* 2013; 23:1460–1465. [PubMed: 23891117]
44. Ye F, Breslow DK, Koslover EF, Spakowitz AJ, Nelson WJ, Nachury MV. Single molecule imaging reveals a major role for diffusion in the exploration of ciliary space by signaling receptors. *Elife.* 2013; 2:e00654. [PubMed: 23930224]

45. Ounjai P, Kim KD, Liu H, Dong M, Tauscher AN, Witkowska HE, Downing KH. Architectural insights into a ciliary partition. *Curr. Biol.* 2013; 23:339–344. [PubMed: 23375896]
46. Dishinger JF, Kee HL, Verhey KJ. Analysis of ciliary import. *Methods Enzymol.* 2013; 524:75–89. [PubMed: 23498735]

Highlights

- A novel system to rapidly and specifically disrupt nucleoporin-dependent transport.
- Forced dimerization of NUP62 attenuates ciliary entry of cytosolic proteins.
- Ciliary transport of membrane proteins is independent of NUP62 dimerization.
- This work extends the parallels between nuclear and ciliary gating mechanisms.

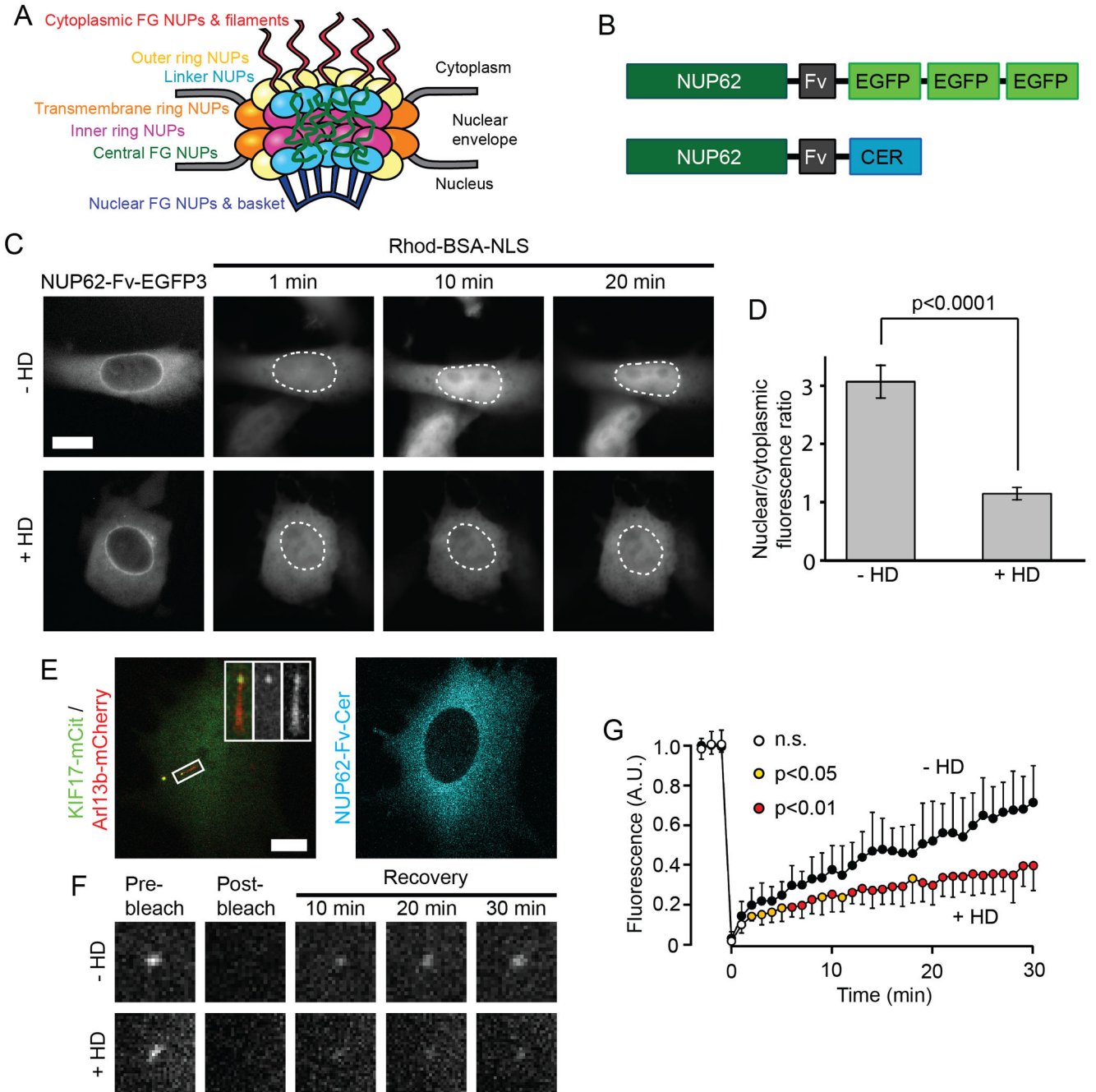


Figure 1. Forced dimerization of NUP62-Fv attenuates active transport into the nuclear and ciliary compartments

(A) Schematic drawing of the NPC based on the model in [10]. Central FG NUPs (shown as green filaments) include NUP62. (B) Schematic drawings of NUP62-Fv-EGFP3 (top) and NUP62-Fv-Cer (bottom) constructs used in this study. See also Figure S1. (C,D) Nuclear import assay. (C) NIH 3T3 cells expressing NUP62-Fv-EGFP3 were microinjected with rhod-BSA-NLS in the absence (top row) or presence (bottom row) of homodimerizer (HD). Representative images are shown. Dashed lines indicate nuclei. Scale bar, 10 μ m. (D) Quantification of nuclear import of rhod-BSA-NLS 20 min after microinjection. Data are

presented as mean \pm SEM. $n = 9$ or 10 cells each. $p < 0.0001$ (t-test). (E–G) Ciliary import assay. (E) Representative images of NIH 3T3 cells expressing KIF17-mCit and Arl13b-mCherry (left, merged) and NUP62-Fv-Cer (right). Insets show magnified images of the boxed region containing the cilium. Scale bar, $5 \mu\text{m}$. (F) Magnified images of KIF17-mCit in the tip of the cilium before and after photobleaching. (G) Normalized fluorescence intensities of KIF17-mCit at the tip of the cilium during the FRAP time course. The first 3 time points are before photobleaching. Data with orange or red circles indicate the time points where fluorescence intensities are significantly different in the presence or absence of HD, with $p < 0.05$ or $p < 0.01$, respectively (t-test). n.s., no significant difference. Error bars show SD. $n = 12$ or 13 cells each.

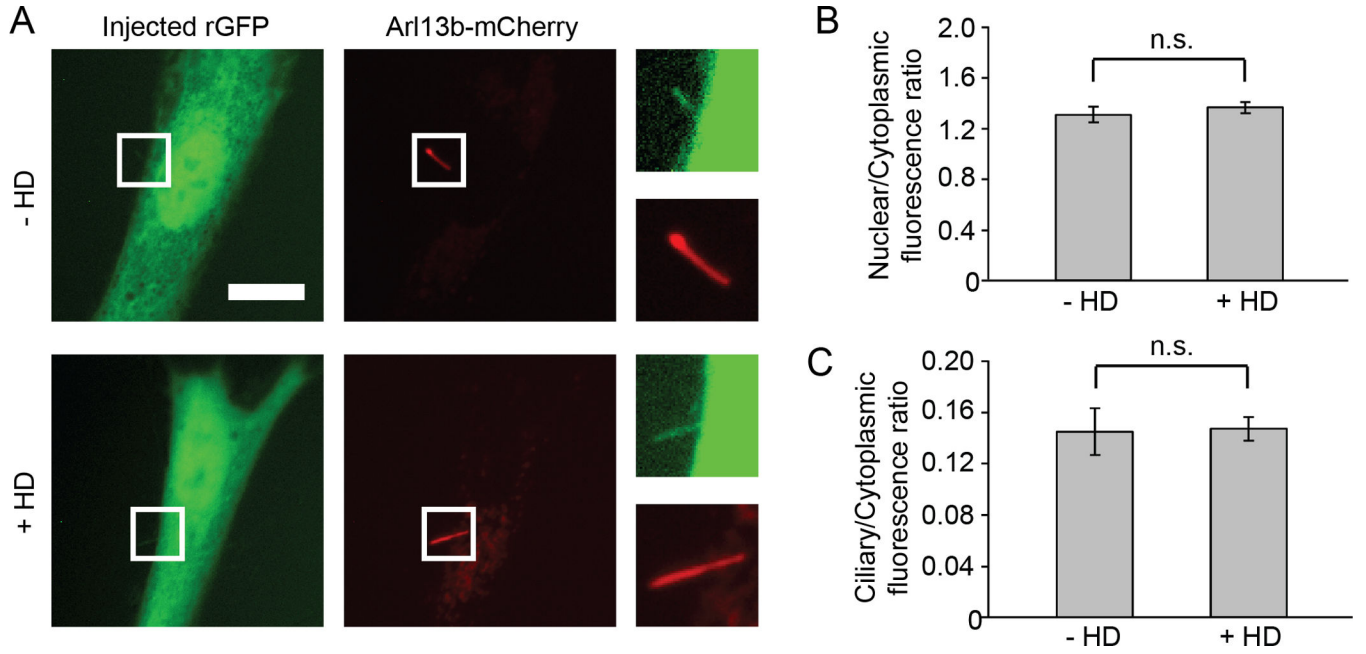


Figure 2. Diffusion of recombinant GFP into ciliary and nuclear compartments is not affected by forced dimerization of NUP62-Fv

(A) NIH 3T3 cells expressing Arl13b-mCherry and NUP62-Fv-Cer (not shown) were microinjected with recombinant GFP (rGFP) in the absence or presence of HD. Representative fluorescence images at 20 min after injection are shown. Magnified images of the cilia are shown on the right of each panel. Scale bar, 10 μ m. (B, C) Quantification of the (B) nuclear/cytoplasmic or (C) ciliary/cytoplasmic fluorescence ratio of injected rGFP in the presence or absence of HD. Fluorescence intensities were measured on images at 20 min after injection. Data are shown as mean \pm SEM ($n = 9$ cells each). n.s., no significant difference by t-test.

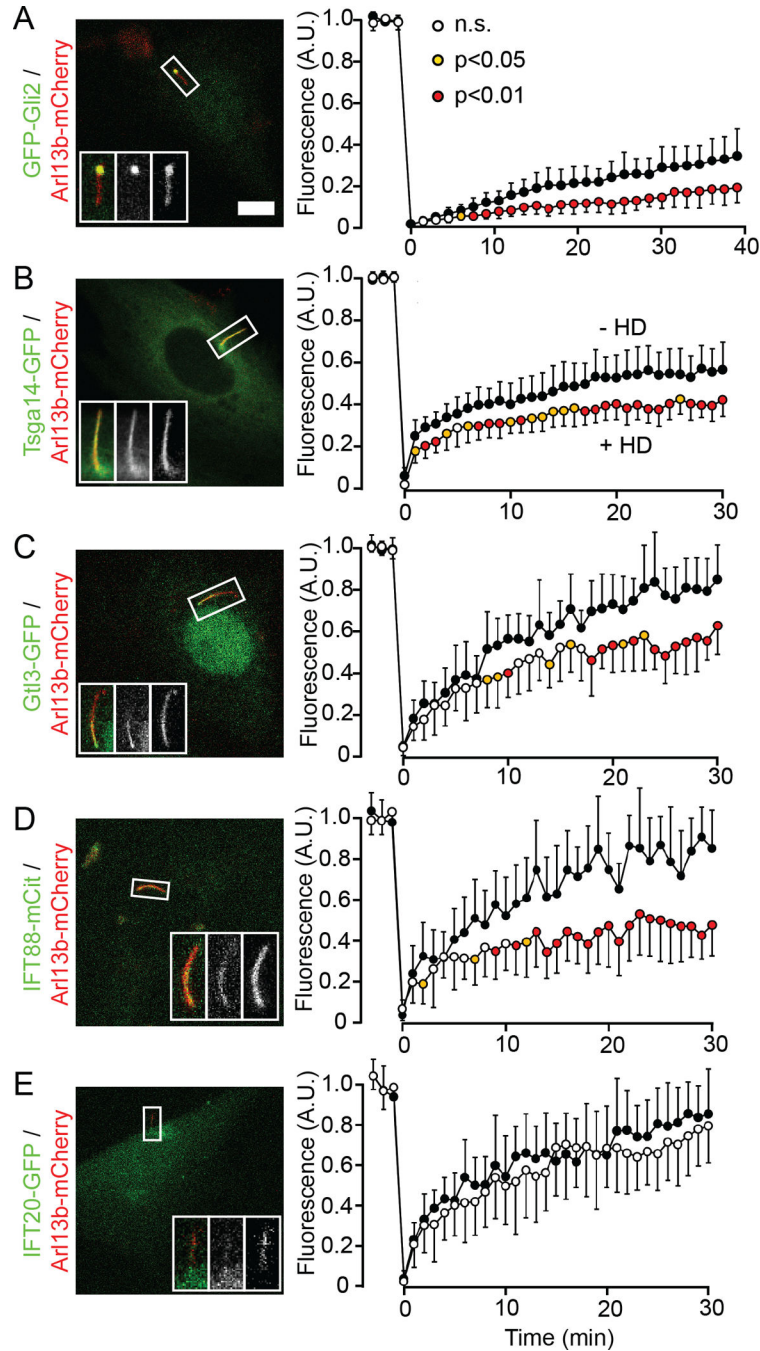


Figure 3. Effect of forced dimerization of NUP62-Fv-Cer on ciliary entry of cytosolic proteins (A–E) (Left column) Representative images of NIH 3T3 cells triple-transfected with a fluorescently-tagged ciliary protein, Arl13b-mCherry, and NUP62-Fv-Cer (not shown). Scale bar, 5 μ m. (Right column) FRAP in the absence (black circles) or presence (white or colored circles) of HD. Data with orange or red circles indicate time points where fluorescence intensities are significantly different in the presence or absence of HD, with $p < 0.05$ or $p < 0.01$, respectively (t-test). n.s., no significant difference. Error bars show SD. See also Figure S3. $n = 10$ – 12 cells each.

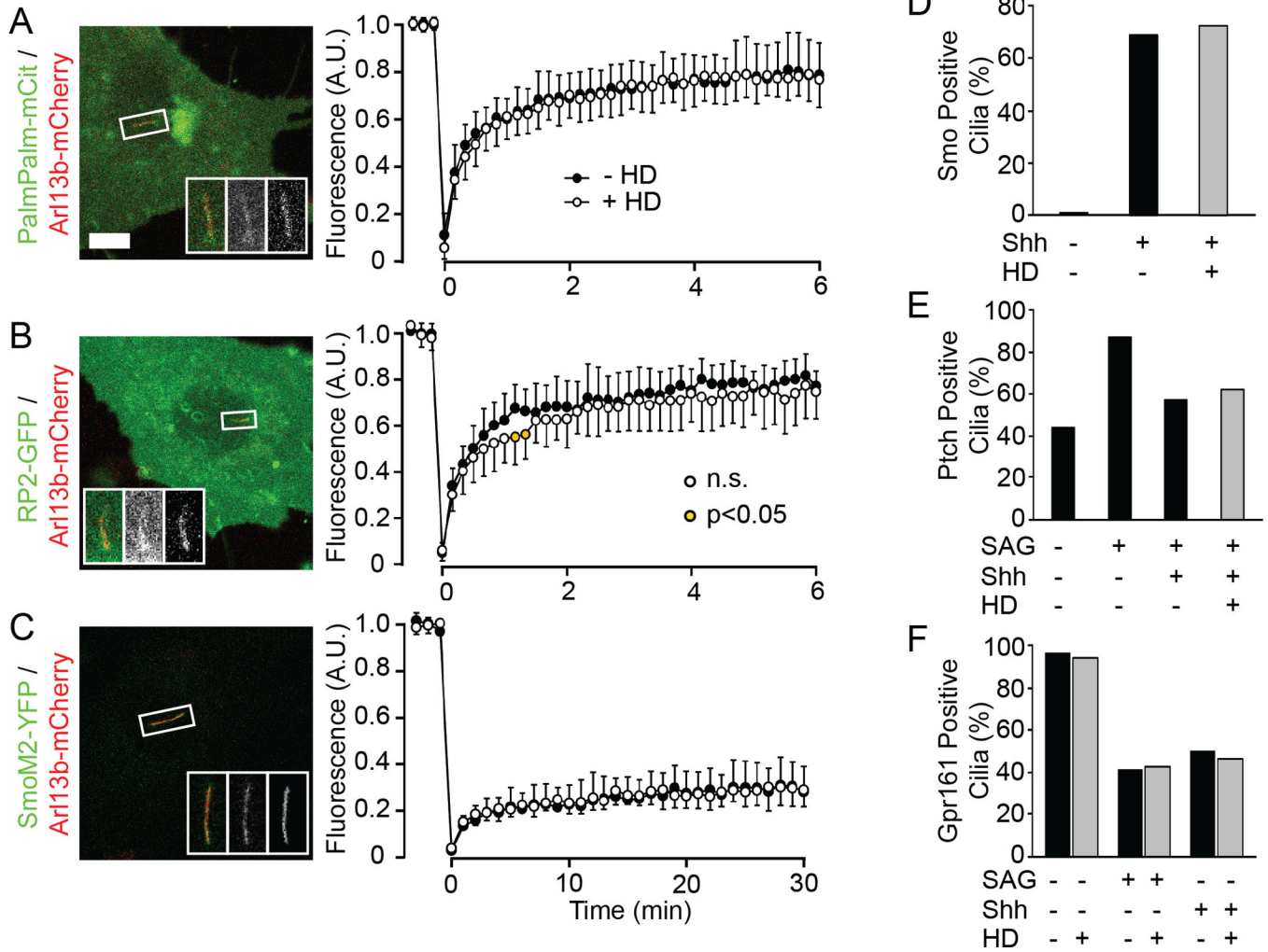


Figure 4. Effect of forced dimerization of NUP62-Fv-Cer on ciliary transport of membrane proteins

(A–C) Representative fluorescence images and FRAP data of peripheral membrane proteins (A, B) and a transmembrane protein (C). Data are shown as in Figure 3. See also Figure S3. $n = 11–13$ cells each. Scale bar, $5 \mu\text{m}$. (D) The percentage of Smo positive cilia was measured in the absence or presence of Shh and/or HD. $n = 50$ cells each. See also Figure S4A. (E) The percentage of Ptch positive cilia was measured in the absence or presence of SAG, Shh and/or HD. Data were obtained from immunofluorescence images. $n = 69–89$ cells. See also Figure S4B. (F) The percentage of GPR161-mCit positive cilia was measured in the absence or presence of SAG, Shh and/or HD. $n = 80$ cells each. See also Figure S4C.